Biosensors and Bioelectronics 50 (2013) 425–430

Contents lists available at SciVerse ScienceDirect

Biosensors and Bioelectronics

journal homepage: www.elsevier.com/locate/bios

Point-of-care protein sensing platform based on immuno-like membrane with molecularly-aligned nanocavities

Chien-Chong Hong [a,*], Chie-Pein Chen [b,*], Jia-Cherng Horng [c], Szu-Yig Chen [d]

[a] Department of Power Mechanical Engineering National Tsing Hua University, Hsinchu 300, Taiwan
[b] Department of Obstetrics and Gynecology, Mackay Memorial Hospital, Taipei 100, Taiwan
[c] Department of Chemistry, National Tsing Hua University, Hsinchu 300, Taiwan
[d] Department of Power Mechanical Engineering National Tsing Hua University, Hsinchu 300, Taiwan

ARTICLE INFO

Article history:
Received 26 April 2013
Received in revised form
8 July 2013
Accepted 9 July 2013
Available online 17 July 2013

Keywords:
Immune-like membrane
Protein biosensor
Microfluidic biochip
Point-of-care platform

ABSTRACT

This paper presents the ability of the novel point-of-care protein sensing platform based on immune-like polymer membrane to separate and sense target analytes in human serum samples using the molecularly-aligned nanocavities. The separation performance of the developed membrane, which is substantially affected by surface chemistry and physics, can be enhanced by alignment of the template molecules. The developed biomimetic membrane with aligned molecular nanocavities can be synthesized and integrated with microfluidic biochips as point-of-care sensing platforms. The measurement results showed that the specific adhesion forces of the developed highly-aligned nanocavities on the immuno-like membranes are comparable to the interaction forces between CRP and biological CRP antibodies. The biomimetic polymer membrane works as antibody to catch specific proteins in complex biofluids within 110 s. The proposed approach is an adaptive technological platform because it facilitates cost-effective mass production and can be applied to a wide range of protein biomarkers.

1. Introduction

Traditional instruments requiring large fluidic samples, complex and lengthy procedures, and professional operators are widely used in clinical laboratories for disease diagnostics. Point-of-care assays based on microfluidic biochips can substantially improve the quality of medical care because of their ease of access, fast response, small bio-sample volume, and portability. A biological enzyme or antibody is the most popular molecular recognition layer for biosensors. Most biochips use biological antibodies with labels for the molecular recognition layers for the optical detection of the target molecules. However, biological antibodies must be stored under −20 °C before use. The affinity may change with time when exposed at room temperature. This reduces the compatibility of the fabrication process to other factors, such as the solvent, process temperature, and interface, for molecular immobilization. In addition, it causes issues with chip integration and storage, which degrades the binding affinity of the antibodies at room temperature, increases uncertainty, limits storage life, and prevents point-of-care applications. Biosensors based on biological molecular recognition techniques are unsuitable for point-of-care clinical diagnostics. Molecular imprinting, referred to as plastic antibody technology, is a novel technique that provides molecular assemblies of desired chemical structures and properties. Based on the concept of "tailor-made," a particular lock is designed to be unlocked by a specific key, mimicking the lock and key model of antigen–antibodies. Molecularly imprinted recognition structures can be artificially synthesized if required. The advantages of such structures include stronger physical and chemical stabilities, long lifecycles, and a low cost. In the presence of a template molecule, functional monomers are polymerized and immobilized complementarily to this molecule. During these processes, a number of functional monomers are assembled in an orderly manner with their functional groups placed at the desired sites within the cavities of the desired size. Therefore, molecular imprinted polymers (MIPs) with binding sites with specific shape and functional group recognition benefit from the high selectivity and high sensitivity sensing in the target molecular compound (Haupt et al., 2000; Bossi et al., 2001).

Biomimetic plastic antibodies based on molecular imprinting are crucial to developing fully integrated microfluidic biochips with biosensors for point-of-care protein testing. As shown in previous studies, molecular imprinted membranes as biosensors have been integrated in microfluidic biochips for detection of small molecules, such as atrazine, glucose, and the propofol anesthetic agent (Piletsky et al., 1995; Malitesta et al., 1999; Hong et al., 2010). Protein imprinted polymers have been examined for the detection of E7 protein

* Corresponding authors.
E-mail addresses: cchong@mx.nthu.edu.tw (C.-C. Hong), cpchen@ms2.mmh.org.tw (C.-P. Chen).

0956-5663/$ - see front matter © 2013 Elsevier B.V. All rights reserved.
http://dx.doi.org/10.1016/j.bios.2013.07.016

(Cai et al., 2010). The specificity in morphology on imprinted nanocavities on a molecular scale has not been addressed in previous studies. In molecular imprinting, the target molecule acts as the template around which the interacting and cross-linking monomers are arranged and co-polymerized to form imprinted nanocavities after polymerization and template removal. The morphology and functional groups of binding sites are strongly related to the selectivity of rebinding the target molecule. Thus, developing immuno-like membranes with efficiently-patterned nanocavities is vital for exhibiting high specificity comparable to biological antibodies. An on-chip molecularly imprinted biosensor was developed for a small molecule (propofol molecule). The polymerization process and the morphology specificity of imprinted nanocavities were examined on a molecular scale (Hong et al., 2012). The influence of surface morphology and alignment of imprinted protein templates on specific interaction force of imprinted functional nanocavities at the nanoscale on the biomimetic immuno-like membranes remains unclear.

C-reactive protein (CRP) is a sensitive marker of inflammation and is primarily synthesized in hepatocytes in response to proinflammatory cytokines, such as tumor necrosis factor alpha and interleukin 6, because of various acute or chronic stimuli (Castell et al., 1990). Elevated serum levels are observed after trauma, tissue necrosis, infection, surgery, and organ failure, and are associated with an increased risk of atherosclerosis, coronary artery disease, stroke, endometriosis, or preterm delivery in pregnancy (Meisner et al., 2006; Makita et al., 2005; Karinen et al., 2005; Orre et al., 2011). The methods used for CRP assay in serum or plasma can be quantitative, semi-quantitative, or qualitative depending on the instruments used. Currently, CRP is measured in clinical laboratories using immunonephelometric or immunoturbidimetric assays (Albrecht et al., 2008). In this work, CRP was used to demonstrate the feasibility of the proposed method. In the near future, plastic-antibody-based biochips can be attached to pre-grammed shape memory polymers for automated fluid operation (Hong and Chen, 2011). The potential applications include cancer diagnostics (Stern et al., 2010), protein–drug interaction (Karlsson et al., 2000), isolation of tumor cells (Yu et al., 2011), and food safety monitoring (Glynn et al., 2006).

Biomimetic immuno-like membranes were developed with aligned molecular nanocavities and compared them with imprinted membranes with random orientation and biological antibodies for surface morphology, alignment degree, and specific interaction force. In addition, the developed membranes were integrated into plastic microfluidic biochips for rapid and precise measurements of CRP in human serum samples (Fig. 1). MIPs for a macromolecule

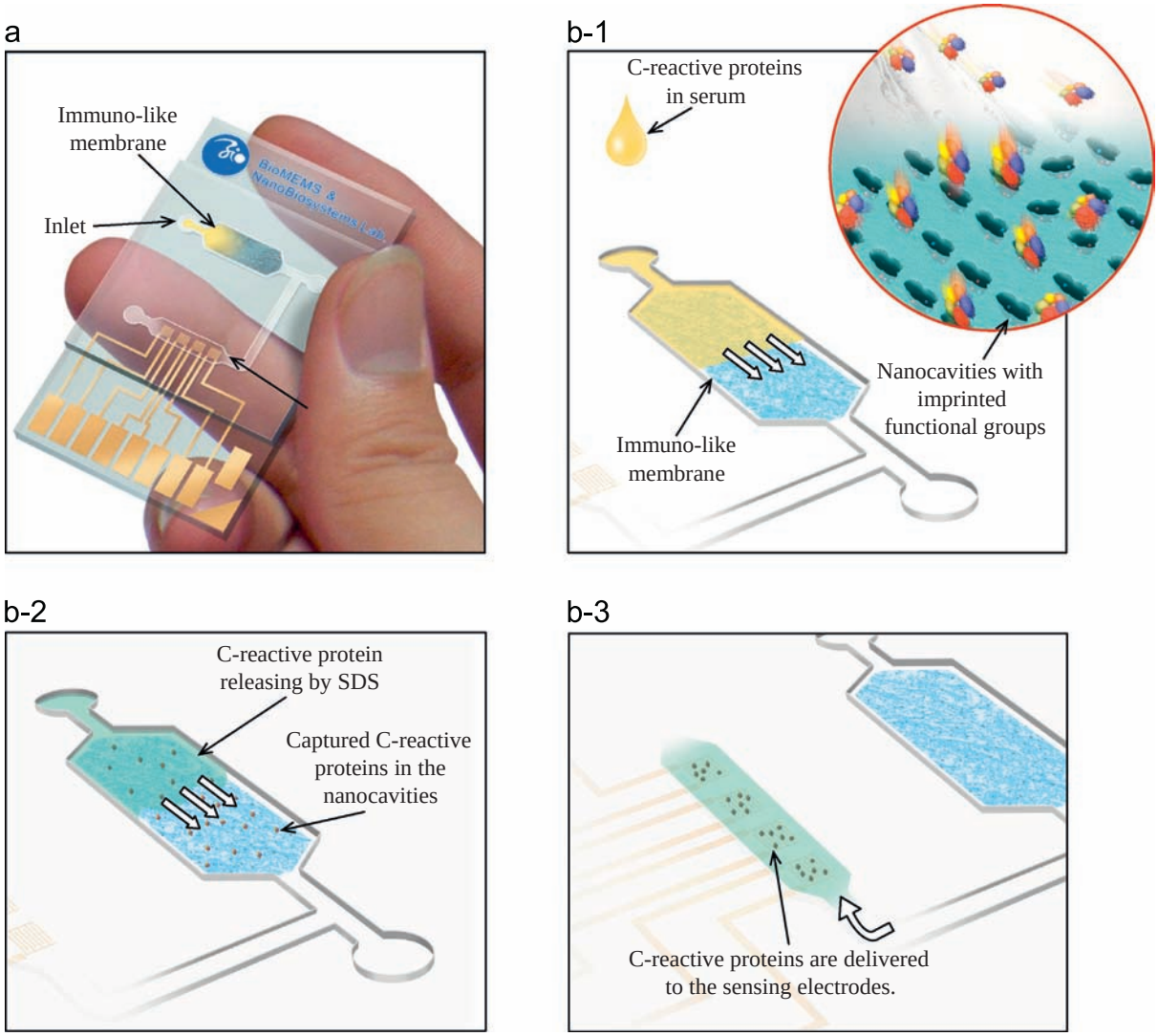

Fig. 1. Schematic illustration of the proposed biomimetic immuno-like membranes with aligned molecular nanocavities for point-of-care protein biosensing. (a) Immuno-like membrane in microfluidic biochips, (b) separation and sensing procedures, (b-1) loading of human serum samples into the microfluidic biochips and capturing CRPs from human serum samples by the immuno-like membrane, (b-2) loading of SDS and releasing of CRPs from the immuno-like membrane, and (b-3) delivery of SDS with CRPs to the electrodes for electronic sensing.

CRP were explored to examine the properties of the molecularly imprinted polymer membranes.

2. Materials and methods

In molecular imprinting, the target molecule acts as the template around which the interacting and cross-linking monomers are arranged and co-polymerized to form imprinted nanocavities after polymerization and template removal. The morphology and functional groups of binding sites are strongly related to the selectivity of rebinding the target molecule. Thus, developing immuno-like membranes with efficiently-patterned nanocavities is vital for exhibiting high specificity comparable to biological antibodies. This work develops a C-reactive protein imprinted polymer film, comprising imprinted nanocavities with unified orientation and distribution formed by removing C-reactive proteins from a polymer membrane, wherein the C-reactive proteins are bound to antibodies on a modified surface. The modified surface is formed by a gold layer on the COC substrate surface binding with cysteamine and glutaraldehyde in order. Imprinted nanocavities with unified orientation and distribution can be easily formed by removing C-reactive protein antibodies from a polymer membrane.

In this work, O-4-nitrophenylphosphorylcholine (O-4NPPC) and polyethylene glycol 400 dimethacrylate (PEG400DMA) were purchased from Sigma-Aldrich. 2,2′-dimethoxy-2-phenyl-acetophenon (DMPA) was purchased from TCI. O-4NPPC was used as a functional monomer, PEG400DMA as a crosslinker and DMPA as an initiator for polymerization. The inhibitor in O-4NPPC and PEG400DMA was removed before use. In this work, cyclic olefin copolymers (Topas® COC 6015, Tg: 150 ° C) were chosen as chip substrates, and they were made into 4 in. plastic wafers by injection molding. The extract solvent are made of 10% sodium dodecyl sulfate and 10% acetic acid.

3. Fabrication of the plastic-based microfluidic biochips with immuno-like membranes

The fabrication steps consist of the fabrication of electronic microfluidic biochips, immuno-like membranes, and the encapsulation of devices. A plastic material, such as cyclic olefin copolymer (COC), was chosen as the substrate. Four inch COC wafers were fabricated using plastic injection molding techniques, and immuno-like membranes were fabricated and integrated in the microfluidic biochips.

The fabrication process of the immuno-like membranes involves three steps: combination, polymerization, and extraction. A monomer (O-4NPPC), was mixed with cross-linker (PEG400DMA), and initiator (DMPA) with a weight ratio of 1:4640:3.4. A template was formed by a gold layer on the COC substrate surface binding with cysteamine, glutaraldehyde, C-reactive protein antibodies, and C-reactive proteins in order. A blank 4-in. COC plastic wafer was prepared and a 25 μm-thick spacer was attached on the template surface. A photolithography mask was placed on the spacer to form a gap between the COC wafer and the mask. The MIP solution was subsequently injected to fill the gap. A UV aligner was applied to perform the polymerization of the plastic antibody solution by UV exposure. The required UV energy for polymerization of 25 μm-thick immuno-like membranes was 17 J/cm^2 (20 mW/cm^2, 850 s). After polymerization of the immuno-like membrane by UV, the imprinted sites were formed as template molecules were released from the immuno-like membrane by the extraction solvent. The immuno-like membrane was patterned on a COC plastic substrate after this procedure (Fig. S2). The microfluidic chip was fabricated with a patterned double-side adhesive tape on a 4 in. blank COC wafer. The immuno-like membrane was subsequently integrated with a plastic microfluidic chamber with a depth of 30 μm. The fabricated device is shown in Fig. 2(a).

4. Experimental results and discussions

4.1. Stability tests of biological CRP antibody

Circular dichroism (CD) measurements were performed using an AVIV Model 410 spectrometer equipped with a Peltier temperature-controlled cell holder using a 1-mm path length quartz cuvette. The protein solutions obtained from Aldrich-Sigma were diluted with D.I. water to a concentration of 25 μM for measurements. Far-UV CD spectra were obtained after incubating the protein solutions at specified temperatures and time. The CD signals were measured every 1 or 2 nm and averaged for 10 s at each wavelength. Thermal unfolding curves were obtained by monitoring the CD signals at 222 nm in a 1-mm path length cuvette with a bandwidth of 1 nm. The CD signal was recorded every 3 °C at a heating rate of 0.6 °C/min. The T_m value was determined by fitting the curve with a simple two-state model, as described in the following equation:

$$\theta(T) = \frac{(a_n + b_n T) + (a_d + b_d T)\exp[-(\Delta H_m/RT)((1/T_m)-(1/T))]}{1 + \exp[-(\Delta H_m/R)((1/T_m)-(1/T))]}$$

where $\theta(T)$ is the observed ellipticities; a_n+b_nT and a_d+b_dT define the folded and unfolded baselines, respectively; ΔH_m is the enthalpy at the unfolding transition; and T_m is the melting temperature.

To examine the thermal stability of the CRP-antibody, its melting temperature (T_m) was measured using CD spectroscopy. The thermal unfolding transition at 222 nm is a cooperative curve (Fig. S1). By fitting the unfolding curve into a simple two-state model, the T_m value was 75 °C. By determining the T_m of the CRP-antibody, the fabrication of the immuno-like membrane was controlled at a temperature that did not destroy the protein structure. Because the immuno-like membrane was manufactured using UV irradiation, which did not result in high temperatures, the conformation of the CRP-antibody was assumed to remain intact.

In addition, a series of CD measurements were performed on the CRP-antibody solutions after various incubation times at 25, 35, and 60 °C to evaluate its structural stability after storage at high temperatures for a long period. As shown in Fig. S1, the far-UV CD spectrum of the CRP-antibody at 25 °C did not change considerably after a 30-day incubation, indicating that the protein is relatively stable at room temperature. By contrast, at temperatures of 35 and 60 °C, the far-UV CD spectrum gradually changed and the CD signals reduced after a 15-day incubation, suggesting that the CRP-antibody is unstable at such high temperatures. Although CD spectroscopy mainly measures the secondary structure of a protein, the CD results can provide valuable information regarding the maximal period that the antibody can remain at high temperatures without changing its native structure. This information also suggests that the analysis of CRP concentration using conventional ESLISA methods may cause antibody decay under warm and hot environments. Thus, the proposed method using a immuno-like membrane can avoid this problem.

4.2. Surface morphology study of imprinted nanocavities

First, the surface morphology of the non-imprinted polymer (NIP), imprinted polymer with random orientations and distribution which was made by spin-coating the template molecules, and the developed immuno-like membranes in which the ordered assembly of template molecules was assisted by the antibody (Fig. S2) were examined using an optical microscope, scanning electron microscope (SEM), and atomic force microscopy (AFM). Both types of MIP membranes have greater surface porosity than NIP membranes (Fig. 2). The aspect ratios

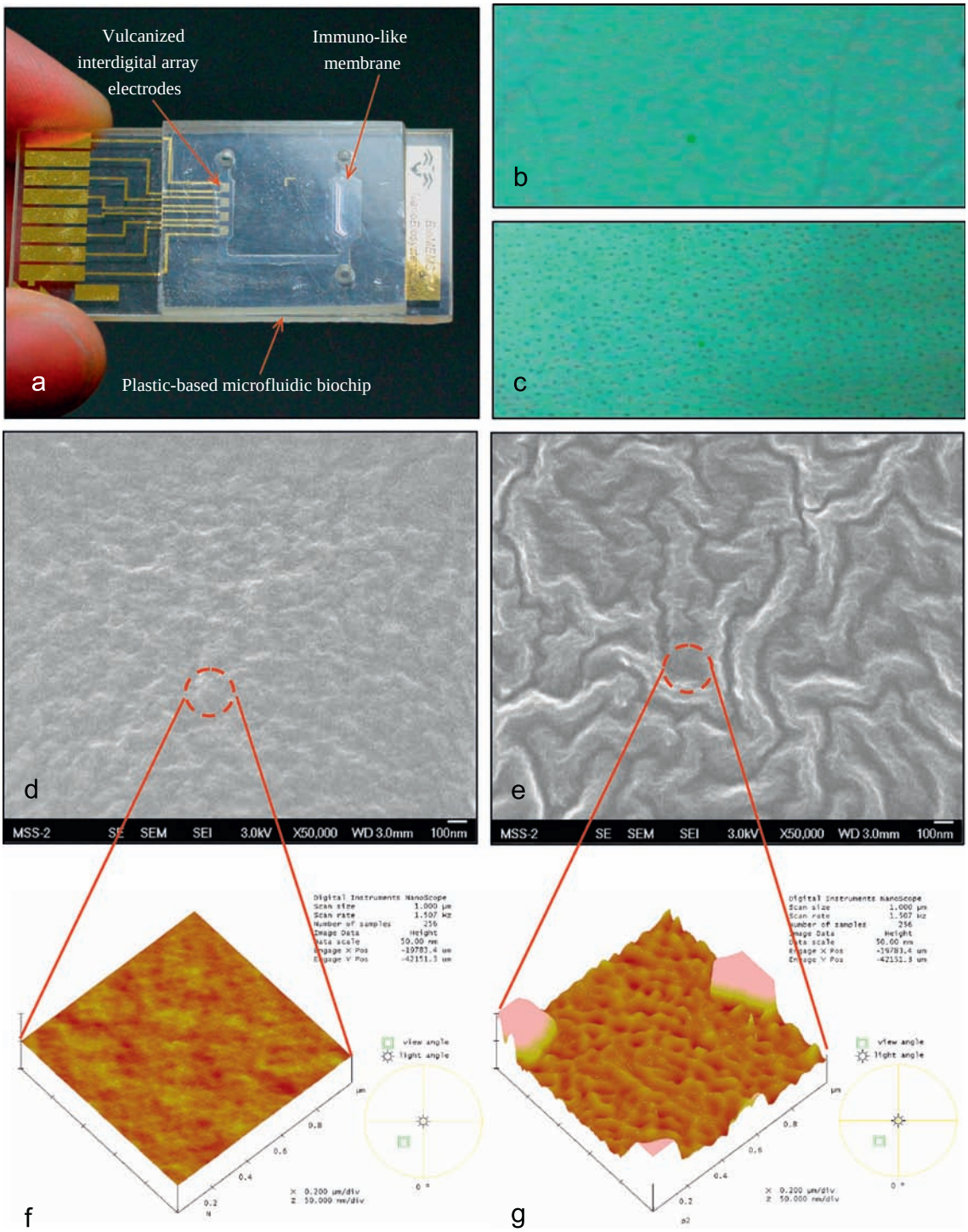

Fig. 2. Photographs of the surface morphology of the developed NIP membranes and immuno-like membranes. (a) Optical image of the immuno-like membrane in the microfluidic biochip, (b) optical image of non-imprinted membrane with high magnification, (c) optical image of immuno-like membrane with high magnification, (d) SEM image of non-imprinted membrane, (e) SEM image of immuno-like membrane, (f) AFM image of non-imprinted membrane, and (g) AFM image of immuno-like membrane.

of the imprinted nanocavities were compared (Fig. 3a and Fig. S3). For non-imprinted polymers, the aspect ratios of the nanocavities on the membrane surfaces were less than 0.018 (Fig. S3a). For imprinted polymers with random orientations and distribution, the aspect ratios of the nanocavities were between 0.029 and 0.067 (Fig. S3b). For the developed immuno-like membranes with aligned nanocavities, the aspect ratios of the nanocavities were between 0.097 and 0.161 (Fig. S3c). The efficiently-aligned nanocavities of immuno-like membranes, which are specific recognition sites formed by the template molecules, exhibited higher anisotropy ratios than the imprinted membranes with random orientations and distribution.

To further examine the specific binding of the imprinted membranes, the adhesion force between nanocavities and CRP antibody-coated AFM tips were measured for various types of imprinted polymers (Fig. 3). The adhesion forces between CRPs and CRP antibodies were 26.86 ± 5.61 nN (Fig. 3c). For non-imprinted polymers, the adhesion forces of the nanocavities were 0.00 nN (Fig. 3d). For imprinted polymers with random orientations, the adhesion

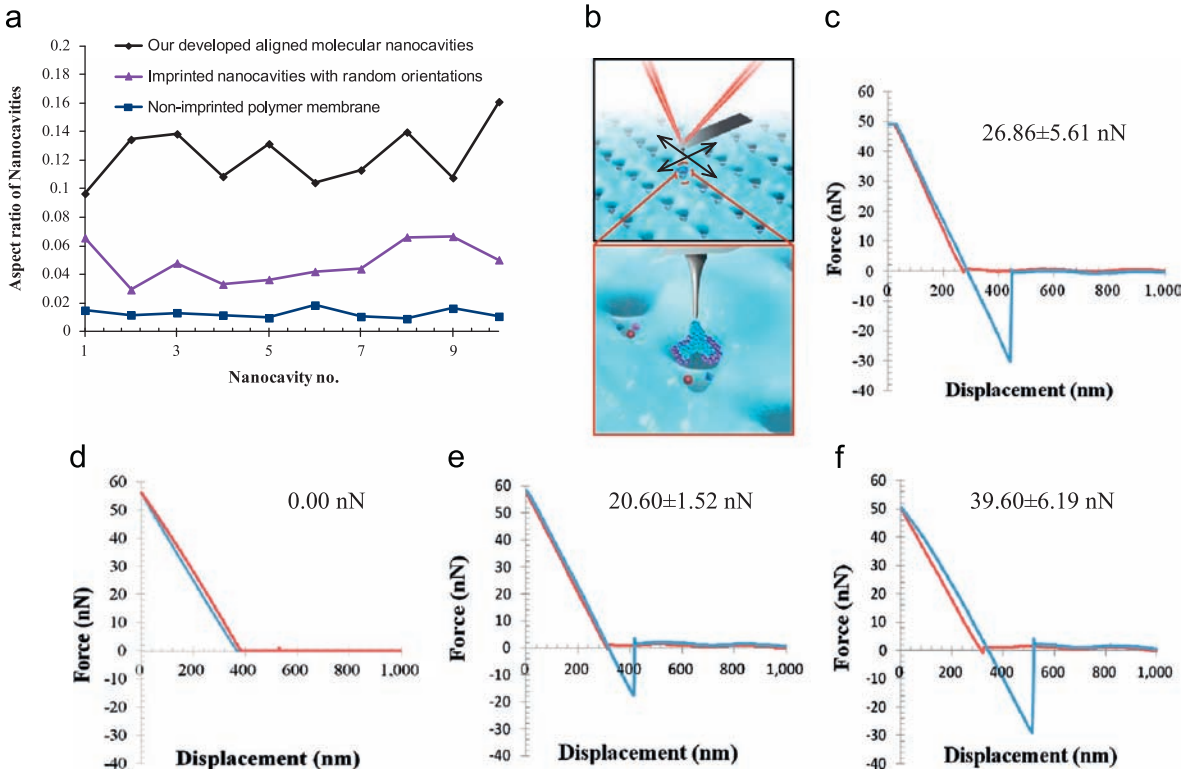

Fig. 3. Adhesion interaction force using AFM for various types of membranes. (a) comparison of aspect ratio of nanocavities on various types of membranes, (b–f) adhesion interaction force measurements, (b) drawing of the setup for measurements within 3×3 adjacent positions (each spacing is 100 nm), (c) biological CRP antibody, (d) NIP membrane, (e) membrane with non-aligned nanocavities, and (f) the developed immuno-like membrane with aligned nanocavities.

forces of the nanocavities were 20.60 ± 1.52 nN (Fig. 3e). For the developed immuno-like membranes with aligned nanocavities, the adhesion forces of the nanocavities were 39.60 ± 6.19 nN (Fig. 3f). The results showed that the specific adhesion forces of the developed highly-aligned (or well-oriented) imprinted nanocavities are 1.47 times higher than the interaction forces between CRP and biological CRP antibodies. Also, the specific adhesion forces of the developed highly-aligned (or well-oriented) imprinted nanocavities are 1.922 times higher than the non-aligned (or random-oriented) imprinted nanocavities.

4.3. Detection of C-reactive proteins

Blood samples are prepared and then detected by ELISA kits and the developed protein sensing platform. Blood from a pregnant woman was collected after written informed consent was obtained, and this study was approved by the Institutional Review Board (IRB) of Mackay Memorial Hospital, Taipei. Blood was collected in 5-mL glass tubes (Becton Dickinson Vacutainer Systems, Franklin Lakes, NJ) containing EDTA for plasma or in plain tubes without anticoagulant for serum during the midtrimester prenatal care visit of healthy pregnant women. Human plasma samples were collected from the EDTA tube and processed using centrifugation at 2000*g* for 20 min within 30 min after blood collection. The contents of collection tubes without anticoagulant were allowed to clot at room temperature for 30 min. Aliquots of maternal plasma or serum were stored at -80 °C until analysis. Each sample was assayed in duplicate.

The following process is for traditional C-reactive protein enzyme-linked immunosorbant assay. Plasma samples were diluted 10,000–200,000-fold with sample diluent prior to analysis. Purified human plasma CRP (Sigma-Aldrich) was used to establish the concentration of CRP in the reference preparations. One-hundred-microliter samples of calibrators (0, 5, 10, 50, 100, 150, and 200 μg/mL), controls, and unknowns were added to the wells of a microtiter plate pre-coated with mouse anti-CRP monoclonal capture antibody (R&D Systems). Human plasma CRP levels or samples of calibrators were evaluated using the DuoSet ELISA development kit (R&D Systems) according to the protocol of the manufacturer. The results were multiplied by the dilution factor (10,000–200,000) and expressed in mg/L.

In additional, sensing studies of the immuno-like membranes were performed using the developed plastic microfluidic biochips. The developed CRP immuno-like membranes were integrated into the plastic-based microfluidic biochips, and subsequently, examined by detecting the CRP concentrations in human serum samples (Fig. 4). Two microliters of spiked human serum sample was delivered to the first microchamber, which contained the immuno-like membrane. After the CRP separation by immuno-like membranes for 90 s, the SDS solvent was delivered to the first microchamber for CRP extraction from the nanocavities on the immuno-like membrane; subsequently, the SDS solvent with the extracted CRP was delivered to the functionalized IDA electrodes for detection. The dynamic discharging curves for various CRP concentrations in human serum were measured from the interdigitated array electrodes (Fig. 4a). The calibration curve was obtained by calculating the discharging time constant from the dynamic voltage curves (Fig. 4b). The CRP samples for the experiments were measured using ELISA kits for comparison (Fig. 4c). Another set of CRP samples was measured and calculated according to the calibration curve (Fig. 4d). The totoal analysis time of the developed system is about 110 s. The immuno-like membrane with molecularly-aligned nanocavities for rapid detection of CRP exhibited excellent performance in the separation and sensing of CRPs.

5. Conclusions

This paper presents the ability of the novel point-of-care protein sensing platform based on immune-like polymer membrane to

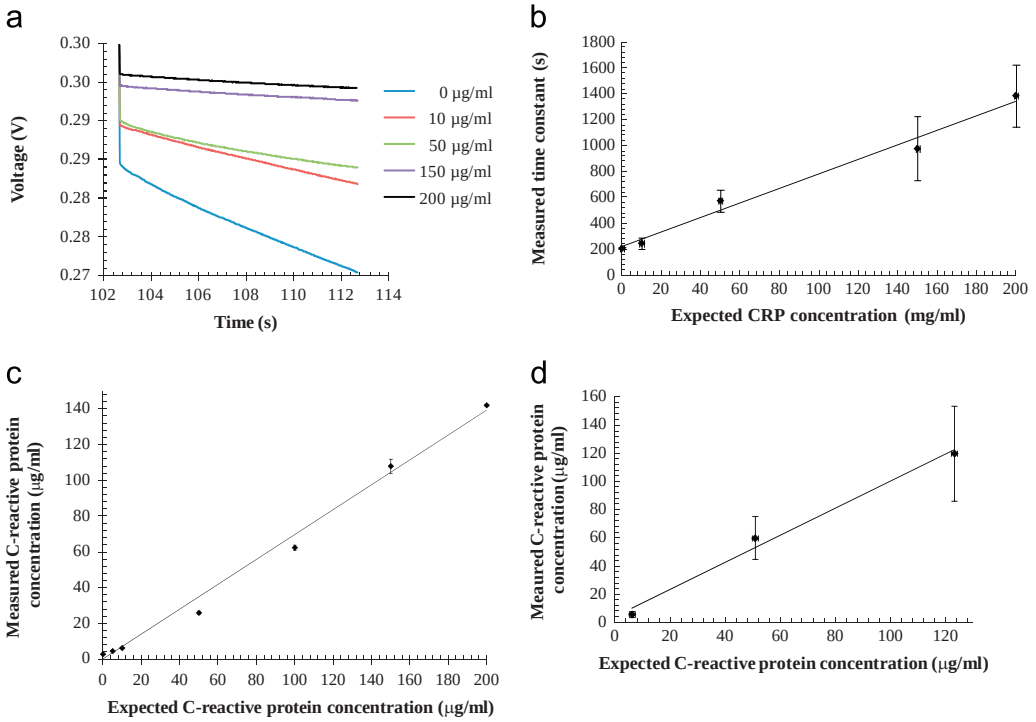

Fig. 4. Comparisons of CRP in human serum samples using ELISA and the developed plastic-based microfluidic biochips with on-chip immuno-like membranes. (a) Dynamic response for various CRP concentrations using the microfluidic biochips with electrical detection, (b) calculated time constant from the dynamic response for various CRP concentrations, (c) ELISA measurement results, and (d) measured and calibrated CRP concentrations using the developed biochips with on-chip immuno-like membranes.

separate and sense target analytes in human serum samples using the molecularly-aligned nanocavities. The performance of the biosensor, which is substantially affected by surface chemistry and physics, can be enhanced by alignment of the template molecules. This study presents potential applications of MIPs beyond their current focus of harvesting the macroscopic scale formation for separation and sensing applications. The measurement results showed that the specific adhesion forces of the developed highly-aligned nanocavities on the immuno-like membranes are comparable to the interaction forces between CRP and biological CRP antibodies. Tradtional ELISA takes several hours for CRP detection. However, our developed point-of-care protein sensing platform takes only 110 s for CRP detection.

The proposed biomimetic immuno-like membrane technology offers several advantages, such as rapid detection, compatible process with BioMEMS and high specificity to CRP in human serum samples, because of the high alignment of macromolecularly imprinted nanocavities. This removes the bottlenecks caused by inferior compatibility with the BioMEMS process, which limits the use of biological antibodies. The novel biomimetic immuno-like membrane incorporates specificity and lifetime into sensing applications in addition to conventional biological antibody use. The potential applications include cancer diagnostics, protein–drug interaction, isolation of tumor cells, and food safety monitoring. Template and plastic antibodies are defined by the MIP process; therefore, they can be tailored to meet specific applications. Finally, the proposed approach is an adaptive technological platform because it facilitates cost-effective mass production and can be applied to a wide range of protein biomarkers.

Acknowledgment

This research was supported by the National Tsing Hua University – Mackay Memorial Hospital Joint Research Projects (98N2451E1 and 100N2737E1) and the National Science Council of Taiwan (NSC 100-2628-E-007-023-MY2). We thank Mr. James Su from the Instrument Technology Research Center for help with the AFM measurements.

Appendix A. Supporting information

Supplementary data associated with this article can be found in the online version at http://dx.doi.org/10.1016/j.bios.2013.07.016.

References

Albrecht, C., Kaeppel, N., Gauglitz, G., 2008. Analytical and Bioanalytical Chemistry 391, 1845–1852.
Bossi, A., Piletsky, S.A., Piletska, E.V., Righetti, P.G., Turner, A.P.F., 2001. Analytical Chemistry 73, 5281–5286.
Cai, D., Ren, L., Zhao, H., Xu, C., Zhang, L., Yu, Y., Wang, H., Lan, Y., Roberts, M.F., Chuang, J., Naughton, M.J., Ren, Z., Chiles, T.C., 2010. Nature Nanotechnology 5, 597–601.
Castell, J.V., Gomez-Lechon, M.J., David, M., Fabra, R., Trullenque, R., Heinrich, P.C., 1990. Hepatology 12, 1179–1186.
Glynn, B., Lahiff, S., Wernecke, M., Barry, T., Smith, T.J., Maher, M., 2006. International Journal of Dairy Technology 59, 126–139.
Haupt, K., Mosbach, K., 2000. Chemical Reviews 100, 2495–2504.
Hong, C.-C., Chang, P.-H., Lin, C.-C., Hong, C.-L., 2010. Biosensors and Bioelectronics 25, 2058–2064.
Hong, C.-C, Chen, J.-C., 2011. Microfluidics and Nanofluidics 11, 385–393.
Hong, C.-C., Lin, C.-C., Hong, C.-L., Chang, P.-H., 2012. Biomedical Microdevices 14, 435–441.
Karinen, L., Pouta, A., Bloigu, A., Koskela, P., Paldanius, M., Leinonen, M., Saikku, P., Jervelin, M.R., Hartikainen, A.L., 2005. Obstetrics and Gynecology 106, 73–80.
Karlsson, R., Kullman-Magnusson, M., Hämäläinena, M.D., Remaeusa, A., Anderssona, K., Borga, P., Gyzanderb, E., Deinumb, J., 2000. Analytical Biochemistry 278, 1–13.
Malitesta, C., Losito, I., Zambonin, P.G., 1999. Analytical Chemistry 71, 1366–1370.
Makita, S., Nakamura, M., Hiramori, K., 2005. Stroke 36, 2138–2142.
Meisner, M., Adina, H., Schmidt, J., 2006. Critical Care 10, R1.
Orre, I.J., Reinertsen, K.V., Aukrust, P., Dahl, A.A., Fossa, S.D., Ueland, T., Murison, R., 2011. Journal of Psychosomatic Research 71, 136–141.
Piletsky, S.A., Piletskaya, E.V., Elgersma, A.V., Yano, K., Karube, I., Parhometz, Y.P., El'skaya, A.V., 1995. Biosensors and Bioelectronics 10, 959–964.
Stern, E., Vacic, A., Rajan, N.K., Criscione, J.M., Park, J., Ilic, B.R., Mooney, D.J., Reed, M.A., Fahmy, T.M., 2010. Nature Nanotechnology 5, 138–142.
Yu, M., Stott, S., Toner, M., Maheswaran, S., Haber, D.A., 2011. The Journal of Cell Biology 192, 373–382.